Acta Cryst D STRUCTURAL BIOLOGY
ISSN 2059-7983

Crystal structures of the disulfide reductase DsbM from *Pseudomonas aeruginosa*

Inseong Jo,[a] Nohra Park,[a] In-Young Chung,[b] You-Hee Cho[b] and Nam-Chul Ha[a]*

[a]Department of Agricultural Biotechnology, Center for Food Safety and Toxicology, Center for Food and Bioconvergence, Research Institute for Agriculture and Life Sciences, Seoul National University, Seoul 08826, Republic of Korea, and [b]Department of Pharmacy, College of Pharmacy, CHA University, Gyeonggi-do 13488, Republic of Korea.
*Correspondence e-mail: hanc210@snu.ac.kr

Received 13 June 2016
Accepted 11 August 2016

Edited by Z. S. Derewenda, University of Virginia, USA

Keywords: disulfide reductase; *Pseudomonas aeruginosa*; DsbM; OxyR; Dsb; glutathione.

PDB references: DsbM, apo, 5hfg; S-glutathionylated, 5hfi

Supporting information: this article has supporting information at journals.iucr.org/d

In bacteria, many Dsb-family proteins play diverse roles in the conversion between the oxidized and reduced states of cysteine residues of substrate proteins. Most Dsb enzymes catalyze disulfide formation in periplasmic or secreted substrate proteins. Recently, a DsbM protein has been found in a Gram-negative bacterium, and was characterized as a cytosolic Dsb member with the conserved C*XX*C motif on the basis of sequence homology to the Dsb-family proteins. The protein was implicated in the reduction of the cytoplasmic redox-sensor protein OxyR in *Pseudomonas aeruginosa*. Here, crystal structures of DsbM from *P. aeruginosa* are presented, revealing that it consists of a modified thioredoxin domain containing the C*XX*C motif and a lid domain surrounding the C*XX*C motif. In a glutathione-linked structure, a glutathione molecule is linked to the C*XX*C motif of DsbM and is bound in an elongated cavity region in the thioredoxin domain, which is also suited for substrate peptide binding. A striking structural similarity to a human glutathione S-transferase was found in the glutathione-binding pocket. Further, biochemical evidence is presented suggesting that DsbM is directly involved in the reduction of the disulfide of Cys199 and Cys208 in OxyR, resulting in the acceleration of OxyR reduction in the absence of reactive oxygen species stress. These findings may help to expand the understanding of the diverse roles of redox-related proteins that contain the C*XX*C motif.

1. Introduction

Proteins with thioredoxin-like folds, such as thioredoxin, glutaredoxin, protein disulfide-bond formation (or isomerization) protein and glutathione S-transferase (GST), are commonly involved in cellular thiol-redox pathways (Qi & Grishin, 2005; Martin, 1995). Among these proteins, protein disulfide-bond formation protein (or isomerase) is crucial for the function and folding of many proteins. In eukaryotes, the disulfide-bond isomerase is located in the endoplasmic reticulum and plays an important role in protein folding (Ellgaard & Ruddock, 2005; Tu & Weissman, 2004). In prokaryotes, a set of proteins, called the Dsb family, catalyze the formation, reduction or isomerization of disulfide bonds in substrate proteins (Ito & Inaba, 2008; Heras *et al.*, 2009; Um *et al.*, 2014, 2015).

To date, many proteins have been identified as members of the Dsb-family proteins in Gram-negative bacteria, which mostly act in the bacterial periplasm. DsbA and DsbL catalyze the formation of disulfide bonds in some periplasmic proteins *via* an oxidative pathway (Chim *et al.*, 2010; Grimshaw *et al.*, 2008; Lester *et al.*, 2015), whereas DsbC and DsbG mediate the reduction or isomerization of protein disulfide bonds in the periplasm *via* a reductive pathway (Yeh *et al.*, 2007; Yoon *et al.*, 2011; Heras *et al.*, 2004). The inner membrane proteins

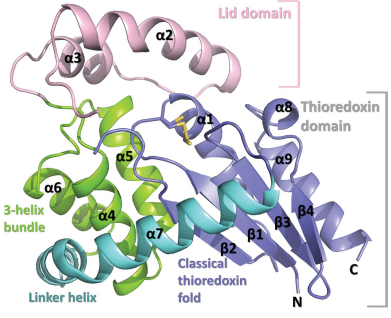

Table 1
X-ray data-collection and refinement statistics.

Values in parentheses are for the highest resolution shell.

	Apo DsbM	S-Glutathionylated DsbM
Data collection		
Beamline	Beamline 5C, Pohang Accelerator Laboratory	
Wavelength (Å)	0.9796	0.9796
Space group	$P4_12_12$	$P4_12_12$
Unit-cell parameters		
a, b, c (Å)	38.8, 38.8, 233.5	39.2, 39.2, 236.8
α, β, γ (°)	90, 90, 90	90, 90, 90
Resolution (Å)	50–1.82 (1.85–1.82)	50–1.80 (1.83–1.80)
No. of unique reflections	17005	18355
$R_{\rm merge}$†	0.076 (0.274)	0.080 (0.473)
$\langle I/\sigma(I)\rangle$	32.8 (4.5)	37.0 (4.2)
Completeness (%)	99.1 (97.7)	99.8 (99.8)
Multiplicity	16.8 (8.4)	12.1 (7.2)
Refinement		
Resolution (Å)	19.99–1.82	19.73–1.80
No. of reflections	16872	18165
$R_{\rm work}/R_{\rm free}$‡	0.184/0.225	0.193/0.244
Total No. of atoms	1680	1703
No. of ligands	0	1
No. of water molecules	96	138
Average B factor (Å^2)	24.0	25.0
R.m.s. deviations		
Bond lengths (Å)	0.006	0.003
Bond angles (°)	0.874	0.695
Ramachandran plot		
Favoured (%)	98.02	98.46
Allowed (%)	1.98	1.54
Outliers (%)	0.0	0.0
PDB code	5hfg	5hfi

† $R_{\rm merge} = \sum_{hkl}\sum_i |I_i(hkl) - \langle I(hkl)\rangle| / \sum_{hkl}\sum_i I_i(hkl)$, where $I_i(hkl)$ is the intensity of the ith observation of reflection hkl and $\langle I(hkl)\rangle$ is the average intensity of the i observations. ‡ $R_{\rm free}$ was calculated using a random set of 10% of reflections that were not used in refinement.

DsbB and DsbI provide oxidizing power to DsbA and DsbL, respectively, in cooperation with ubiquinone. In contrast, the inner membrane protein DsbD keeps DsbC in its reduced state (Inaba & Ito, 2008; Grimshaw *et al.*, 2008). A newly characterized gene (PA0058) in *Pseudomonas aeruginosa* showed the highest sequence similarity to DsbA1 from *P. aeruginosa* (with a sequence identity of 14%), and was designated DsbM (Wang *et al.*, 2012). Owing to the lack of a signal sequence for secretion, DsbM seemed to be a cytosolic member of the Dsb family of proteins (Wang *et al.*, 2012). *P. aeruginosa* DsbM showed disulfide-reducing activity *in vitro*, similar to the periplasmic proteins DsbC and DsbG. Oxidized DsbM was found to be reduced by cellular glutathiones. Furthermore, DsbM has been implicated in the reduction of the peroxide-dependent transcription factor OxyR in the bacterial cytoplasm (Li *et al.*, 2014; Wang *et al.*, 2012).

OxyR has two redox states depending on the presence of hydrogen peroxide. In the presence of hydrogen peroxide, OxyR undergoes a conformational change to its active state by the formation of a disulfide bond between two conserved cysteine residues. In the absence of hydrogen peroxide, OxyR returns to its reduced form (inactive state) through cellular reducing agents, such as glutathione (Toledano *et al.*, 1994; Storz & Tartaglia, 1992; Jo *et al.*, 2015; Choi *et al.*, 2001). The interaction between DsbM and OxyR was confirmed through a yeast two-hybrid screen, and DsbM showed increased reduction of OxyR in *P. aeruginosa* (Li *et al.*, 2014; Wang *et al.*, 2012). In particular, it was reported that aminoglycoside resistance was increased in *P. aeruginosa* when *dsbM* was deleted. However, the relationship between the two proteins remains ambiguous because the structure and function of DsbM are still largely unknown. In this study, we determined crystal structures of DsbM from *P. aeruginosa* and subsequently carried out biochemical studies based upon the structures.

2. Experimental procedures

2.1. Plasmid construction

DNA encoding DsbM was amplified from *P. aeruginosa* PAO1 and inserted into the pProEx-HTa vector (Invitrogen, USA) containing a hexahistidine tag and a *Tobacco etch virus* (TEV) protease cleavage site upstream of the multiple cloning site. To express the DsbM C14S and C17S mutants, site-directed mutagenesis was performed with the pProEx-HTa:: *PaDsbM* plasmid (Landt *et al.*, 1990). To express the PaOxyR C199S/C208S/C296S, C25S/C208S/C296S and C25S/C199S/C296S mutants, we used the previously described vector pET15H::*oxyR* (Heo *et al.*, 2010).

2.2. Protein purification

Cleavable N-terminally hexahistidine-tagged DsbM variants were expressed in the *Escherichia coli* BL21 (DE3) strain as described previously (Jiao *et al.*, 2013). The *E. coli* BL21 (DE3) strain transformed with each recombinant plasmid was cultured in LB medium at 37°C until the OD_{600} reached 0.6, and protein expression was then induced by adding 0.5 m*M* isopropyl β-D-1-thiogalactopyranoside (IPTG) for 6 h at 30°C. The harvested cells were resuspended in 50 ml resuspension buffer consisting of 20 m*M* Tris–HCl buffer pH 8.0, 150 m*M* NaCl, 2 m*M* β-mercaptoethanol and disrupted by one pass through a French press at a pressure of 138 MPa. The DsbM variant proteins were purified by Ni–NTA chromatography and the N-terminal His tag was cleaved using TEV protease. The proteins were further purified using anion-exchange chromatography (HiTrap Q, GE Healthcare, USA) and size-exclusion chromatography (HiLoad 26/600 Superdex 200 pg, GE Healthcare, USA) equilibrated with 20 m*M* Tris–HCl pH 7.5, 150 m*M* NaCl, 2 m*M* tris(2-carboxyethyl)phosphine (TCEP). Purified proteins were concentrated to 30 mg ml^{-1} and stored at −75°C.

The OxyR variants were expressed in *E. coli* BL21 (DE3) and purified as described previously (Jo *et al.*, 2015). In brief, the OxyR variants were expressed at 30°C and purified in two chromatographic steps using an Ni^{2+}–NTA agarose column and size-exclusion chromatography.

2.3. Crystallization, data collection and structural determination of DsbM

The initial crystallization condition for DsbM was identified using a commercial screen (PEG/Ion, Hampton Research) by

the sitting-drop vapour-diffusion method at 14°C. To obtain high-quality crystals, we optimized the crystallization condition and crystallization method. Finally, plate-shaped crystals (100 × 20 × 1 µm) of apo DsbM were obtained in precipitant solution consisting of 0.1 *M* bis-tris–HCl pH 6.5, 1%(*v*/*v*) Tacsimate pH 6.5 (Hampton Research), 2 m*M* TCEP, 20%(*w*/*v*) PEG 3350 using the hanging-drop vapour-diffusion method at 14°C. Crystals appeared in 2–3 weeks. To obtain crystals of S-glutathionylated DsbM, crystals were soaked in precipitant solution consisting of 0.1 *M* bis-tris–HCl pH 6.5, 1%(*v*/*v*) Tacsimate pH 6.5 (Hampton Research), 20%(*w*/*v*) PEG 3350 with 5 m*M* oxidized glutathione (GSSG).

The crystals were flash-cooled in a nitrogen stream at −173°C using Paratone N oil as a cryoprotectant. X-ray diffraction data were collected on beamline 5C at Pohang Accelerator Laboratory and were processed with the *HKL*-2000 package (Otwinowski & Minor, 1997). The crystal of apo DsbM belonged to space group $P4_12_12$, with unit-cell parameters a = 38.8, b = 38.8, c = 233.4 Å (Table 1). The structure of apo DsbM was determined by the molecular-replacement method using *MOLREP* in the *CCP*4 package (Winn *et al.*, 2011). The structure of a putative protein disulfide isomerase (PDB entry 2in3, 26% sequence identity; Midwest Center for Structural Genomics, unpublished work) was used as a search model. The final structure of apo DsbM was refined at 1.82 Å resolution with an R factor of 19.4% and an R_{free} of 24.3% using *phenix.refine* (Afonine *et al.*, 2012). The S-glutathionylated DsbM crystal also belonged to space group $P4_12_12$, with unit-cell parameters a = 39.2, b = 39.2, c = 236.8 Å (Table 1). The final structure of S-glutathionylated DsbM was refined at 1.80 Å resolution with an R factor of 20.0% and an R_{free} of 24.3%. The ligand was manually fitted to the initial $F_o - F_c$ map, which showed clear structural features for the S-glutathionylated cysteine residue (Supplementary Fig. S1).

2.4. Obtaining mixed-disulfide intermediates between DsbM and the OxyR peptide

The OxyR peptide ($GHC^{199}FRDQVL$) was synthesized and reacted in the presence of Ellman's reagent [5,5′-dithiobis-(2-nitrobenzoic acid)] to form an interpeptide disulfide bond between the Cys199 residues of the peptides (PEPTRON, Daejeon, Republic of Korea). To obtain the mixed-disulfide intermediate between DsbM and the oxidized OxyR peptide, 20 µ*M* DsbM C17S variant was incubated in 20 m*M* Tris–HCl pH 7.5 containing 40 µ*M* OxyR peptide at room temperature for 10 min; 4–20% gradient polyacrylamide gels (Bio-Rad) were used to perform SDS–PAGE and were stained with Coomassie Blue.

2.5. Redox-potential determination using tryptophan fluorescence spectroscopy

Purified wild-type DsbM protein at 120 µ*M* was equilibrated with various ratios of reduced DTT (1,4-dithiothreitol) and oxidized DTT (*trans*-4,5-dihydroxy-1,2-dithiane) for 6 h at 298 K in degassed buffer consisting of 50 m*M* Tris–HCl pH 7.0, 0.5 m*M* EDTA. The total concentration of reduced DTT and oxidized DTT was fixed at 10 m*M* and the values of $[GSH]^2/[GSSG]$ were adjusted to 1.98, 9.8×10^{-1}, 3.1×10^{-1}, 1.2×10^{-1}, 8.1×10^{-2}, 3.2×10^{-2}, 5.0×10^{-3}, 1.9×10^{-3}, 1.1×10^{-4} and 1.0×10^{-6} *M*. To calculate the portion of reduced DsbM, tryptophan fluorescence was measured with an excitation wavelength of 295 nm and an emission wavelength range of 300–400 nm. This experiment indicated that the fluorescence of Trp16 depends on the ratio of GSH and GSSG. The redox potentials were calculated from the emission values at 354 nm wavelength as reported previously (Shukla *et al.*, 2014). The midpoint redox potential (E_m) of DsbM was calculated by fitting the measured data to the Nernst equation $E = E^0 - (RT/nF)\ln([GSH]^2/[GSSG])$ (Shukla *et al.*, 2014; Jones, 2002). E^0 is the standard redox potential (E^0 = −240 mV for GSH/GSSG at pH 7.0; Schafer & Buettner, 2001), R is the universal gas constant (R = 8.31 J K^{-1} mol^{-1}), T is the temperature (T = 298 K), n is the number of moles of electrons transferred (n = 2 for GSH/GSSG) and F is the Faraday constant ($F = 9.65 \times 10^4$ C mol^{-1}).

2.6. Reductase assay of DsbM using TNB-labelled OxyR mutants

For the reductase assay, TNB-labelled OxyR mutants (C199S/C208S/C296S, C25S/C208S/C296S and C25S/C199S/C296S) were prepared at 10 µ*M* as described previously (Yoon *et al.*, 2014). The concentrations of the TNB-labelled proteins were measured as released TNB^{2-} by treatment with 100 m*M* DTT for 30 min at room temperature. In the reductase assay, the TNB-labelled OxyR mutants were mixed with 50 µ*M* DsbM protein or 50 µ*M* glutathione at room temperature. The absorbance of the released TNB^{2-} was measured at 412 nm (Ellman *et al.*, 1961).

3. Results

3.1. Structural determination of DsbM

We overproduced full-length *P. aeruginosa* DsbM protein (apo form; ∼25 kDa) using an *E. coli* expression system and obtained plate-shaped crystals. To prepare S-glutathionylated DsbM crystals, oxidized glutathione was incubated with the apo-form DsbM protein crystals. Crystal structures of apo and S-glutathionylated DsbM, both belonging to space group $P4_12_12$, were determined at 1.82 and 1.80 Å resolution, respectively. The crystallographic asymmetric unit of both crystals contained one protomer. The X-ray diffraction data-collection and refinement statistics are summarized in Table 1.

3.2. Overall structure of DsbM

The molecular size of *P. aeruginosa* DsbM measured using size-exclusion chromatography suggested that DsbM behaves as a monomer or a dimer in solution (Supplementary Fig. S1). The crystal structure of *P. aeruginosa* DsbM indicated that it is a monomeric protein from the shallow packing interactions between the protomers in the crystal. The crystal structures revealed that DsbM is composed of two distinct domains: a

thioredoxin domain and a lid domain. The thioredoxin domain consists of a classical thioredoxin fold, a three-helix bundle and a linker α-helix (Fig. 1). The classical thioredoxin fold (light purple) was constructed by β1–β4, α1, α8 and α9, which contain the core C*XX*C motif (Cys14-Gly15-Trp16-Cys17) in the N-terminus of helix α1 (Qi & Grishin, 2005; Shouldice *et al.*, 2011). The three-helix bundle is composed of helices α4–α6 (green) and is linked to the thioredoxin fold by a long linker α-helix α7 (cyan). The lid domain (α2–α3; pink) is inserted between β2 and α4 in the thioredoxin domain and covers the C*XX*C motif of the thioredoxin domain (Fig. 1).

3.3. Structural comparison with GST and DsbA

We performed a three-dimensional structure-based comparison against the PDB using the *DALI* server (Holm & Rosenström, 2010). A putative protein disulfide isomerase from *Nitrosomonas europaea* (NePDI; PDB entry 2in3, 26% sequence identity) had the highest *Z*-score of 24.0. All parts of the NePDI structure were comparable with those of the DsbM structure, with an r.m.s. deviation of 2.2 Å for 153 matched C^{α} atoms (Figs. 2*a* and 2*d*). Unfortunately, no further study related to the function of this protein has been reported to date. A κ-class human glutathione S-transferase (hGSTκ; PDB entry 3rpn; Wang *et al.*, 2011) ranked second (*Z*-score 17.5; sequence identity 14%) and showed a striking structural similarity, although hGSTκ does not contain the C*XX*C motif (Qi & Grishin, 2005). The DsbM structure was superimposable on the hGSTκ structure (r.m.s. deviation of 3.8 Å for 153 C^{α} atoms), with a divergence in the lid domains of the two proteins. The r.m.s. deviation between the two proteins was reduced to 2.1 Å for 100 C^{α} atoms when the lid domain was removed from the comparison (Fig. 2*b*).

Notably, DsbA proteins were also found in the *DALI* search, with a *Z*-score range of 10–13. DsbA from *P. aeruginosa* (sequence identity 14%; PDB entry 3h93; Shouldice *et al.*, 2011) showed the best match among them (r.m.s. deviation of 3.1 Å for 78 C^{α} atoms). However, DsbA proteins do not possess the lid domain (Fig. 2*c*) and contain an N-terminal signal sequence for secretion to the periplasm (Fig. 2*d*).

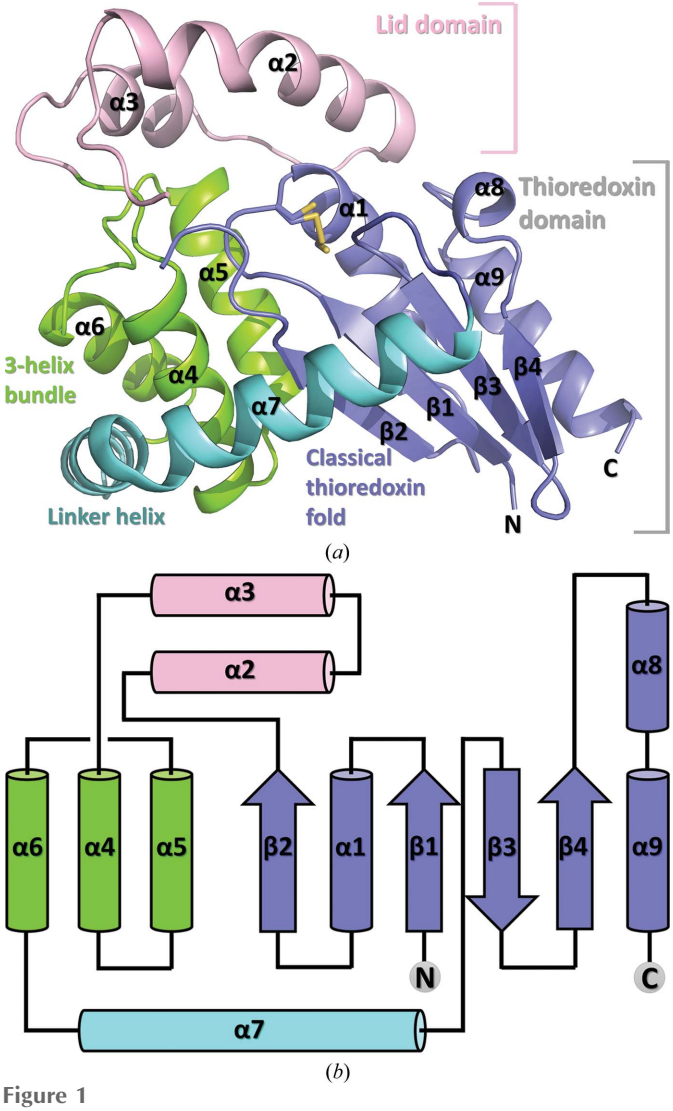

Figure 1
Overall structure of DsbM. (*a*) Ribbon representation of the apo DsbM structure. DsbM comprises a lid domain (violet) and a thioredoxin domain consisting of the classical thioredoxin domain (light purple), a three-helix bundle (green) and a linker helix (cyan). (*b*) The folding topology of DsbM. The labelling and colouring of the secondary-structural elements are the same as in (*a*).

3.4. The active-site C*XX*C motif

Dsb-family proteins contain the C*XX*C motif, which contains key residues for their function. In the structure of apo DsbM, the cysteine residues in the DsbM ^{14}C*XX*C^{17} motif exhibited mixed conformations of the reduced and oxidized states (Fig. 3*a* and Supplementary Fig. S2). However, we cannot exclude the possibility that DsbM was oxidized during data collection. Cys14 S^{γ} shifted towards the main-chain NH of α1 in the reduced conformation, which may be the result of a decrease in the pK_a of Cys14 owing to the effects of the α-helix dipole (Fig. 3*c*; Kortemme & Creighton, 1995). In the oxidized conformation, the Cys14 S^{γ} atom was adjacent to the main-chain NH of Cys17 rather than those of Gly15 and Trp16 as a result of the disulfide bond between Cys14 and Cys17 (Fig. 3*d*). In addition, three water molecules (w1, w2 and w3) were trapped by the NH backbone of Phe177 and the side chains of Cys14 and Gly15 (Figs. 3*c* and 3*d*).

A CGWC sequence was found in the C*XX*C motif of DsbM, in which the Trp16 residue facilitates a hydrophobic interaction of Ile66 and Leu69 of the lid domain with other hydrophobic residues between the two domains (Fig. 3*a*). A conserved *cis*-proline loop (Gly176-Phe177-Pro178) was also observed, which is known to be related to decreases in the pK_a value of a redox-active cysteine and interactions with substrates among the thioredoxin-family proteins (Figs. 2*d* and 3*b*; Charbonnier *et al.*, 1999; Kurth *et al.*, 2014).

3.5. The glutathione-binding site and its implications for substrate binding

The crystal structure of DsbM in complex with glutathione has implications not only for how DsbM recognizes glutathione but also for how it recognizes the substrate proteins. In

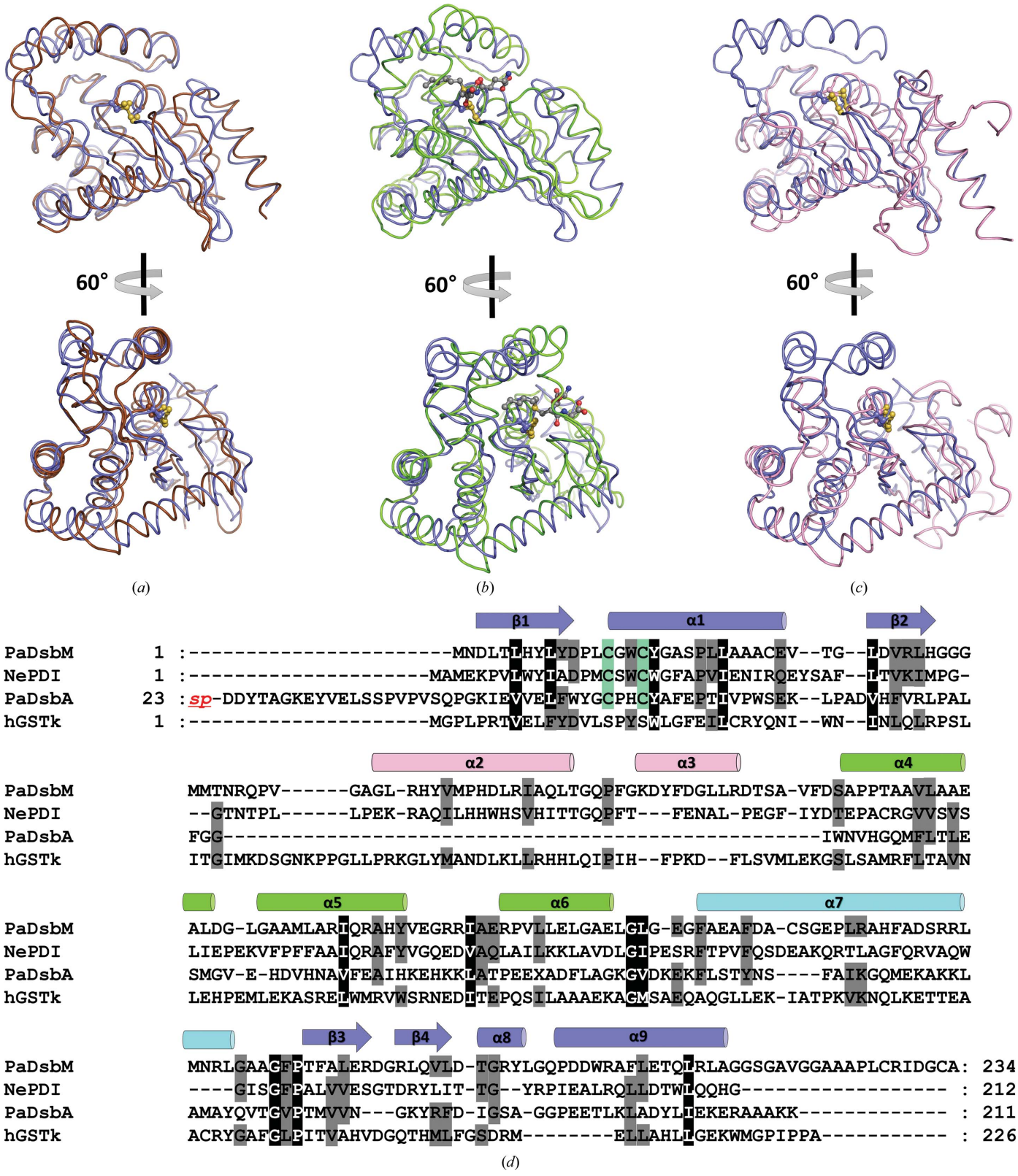

Figure 2
Structural comparison of DsbM. (*a*) Superposition of DsbM (light purple) and *N. europaea* PDI (brown). The catalytic cysteines in the thioredoxin fold are represented as ball-and-stick models. (*b*) Superposition of DsbM (light purple) and human GST*κ* (green). The ball-and-stick representations show the catalytic cysteines (light purple) of DsbM. (*c*) Superposition of DsbM (light purple) and DsbA from *P. aeruginosa* (violet). The catalytic cysteines in the thioredoxin fold are represented as ball-and-stick models. (*d*) Structure-based sequence alignment. PaDsbM, *P. aeruginosa* DsbM; NePDI, *N. europaea* putative protein disulfide isomerase; PaDsbA, *P. aeruginosa* DsbA; hGSTk, human GST*κ*. The secondary-structural elements are shown above the sequence with the same colour code as in Fig. 1. The cysteine residues of the C*XX*C motif are shaded in green. The signal peptide (*sp*) in PaDsbA is omitted.

the glutathione-linked (or S-glutathionylated) DsbM structure, the cysteine residue in the glutathione (L-γ-glutamyl-L-cysteinyl-glycine) is covalently linked to Cys14 in the C*XX*C motif *via* a disulfide bridge (Fig. 3*b*). The glutathione molecule is located in a shallow elongated pocket in the thioredoxin domain near Cys14, which is lined by Trp16 of the C*XX*C motif, Phe177 and Pro178 (Fig. 3*b*). The side chain of Trp16 makes hydrophobic contacts with the backbone of the γ-glutamyl moiety of glutathione, which is also observed in the structure of glutathione-bound human GSTκ (Fig. 3*b*; Wang *et al.*, 2011). The backbone amide and carboxyl groups of Phe177 in the *cis*-proline loop form two hydrogen bonds to the carboxyl and amide groups of the cysteine moiety of glutathione, respectively (Fig. 3*b*).

The glutathione-binding site of DsbM is further extended in both directions, forming a long groove between the thioredoxin domain (grey) and the lid domain (pink) with open ends (Fig. 4). The C*XX*C motif (green) is present in the centre of the groove (Fig. 4*a*). The width and height of the groove are approximately 30 and 12 Å, respectively (Fig. 4*a*). In contrast, the glutathione-binding site of GST is smaller and closed at both ends and fits the glutathione molecule for more extensive interactions, especially at the end regions (Fig. 4*b*; Wang *et al.*, 2011). Thus, these findings suggest that the glutathione-

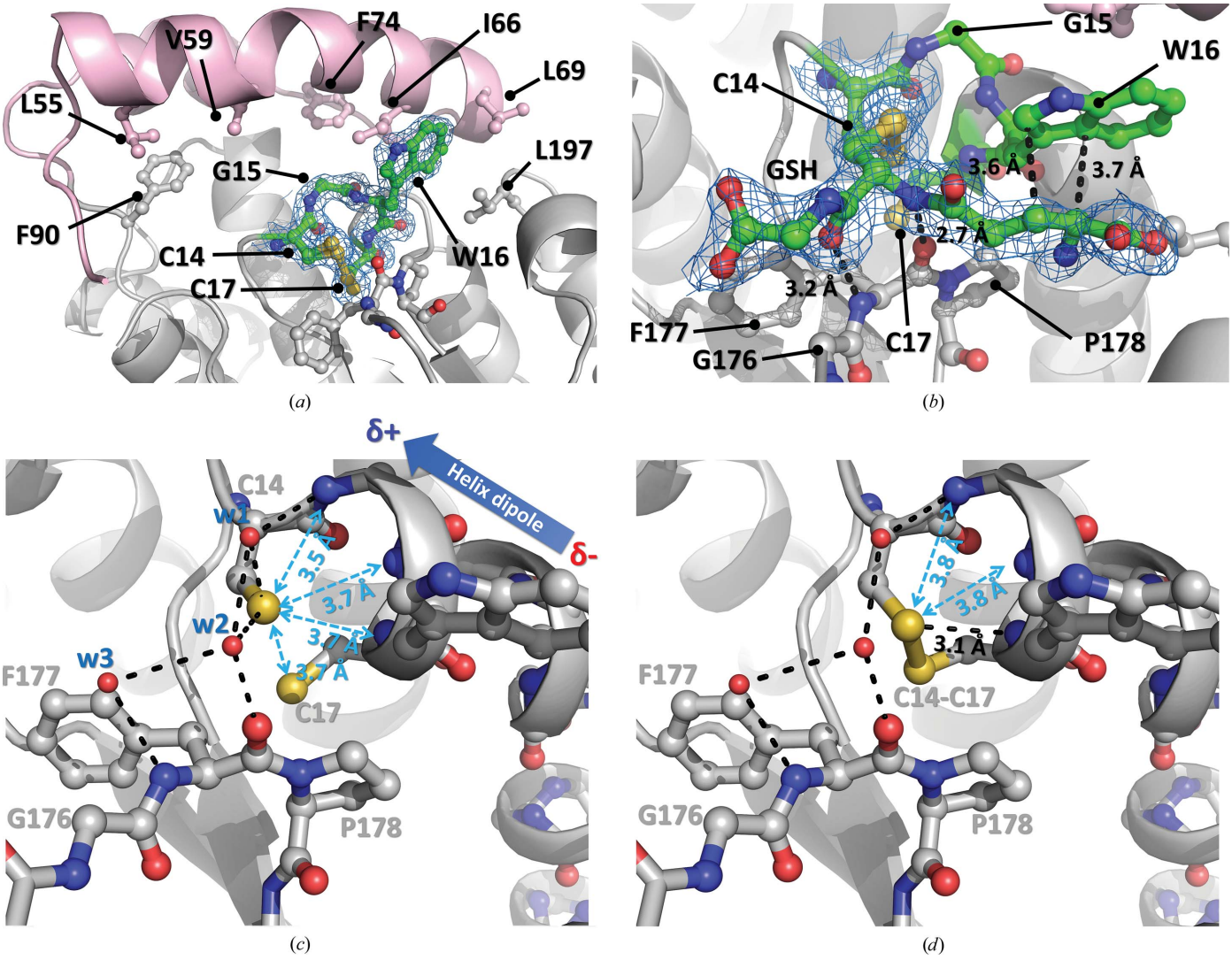

Figure 3
Structural details of the active site. (*a*) The structure of the ^{14}C*XX*C^{17} motif (ball-and-stick model in green) and the surrounding environment of apo DsbM. The reduced and oxidized forms of Cys14 and Cys17 coexist (see Supplementary Fig. S2) and are fitted to a $2F_o - F_c$ electron-density map contoured at 1.0σ (blue mesh). The residues involved in the hydrophobic interaction between the lid domain (salmon) and the thioredoxin domain (grey) are shown in stick representation and labelled. (*b*) The glutathione-linked ^{14}C*XX*C^{17} motif (green) in S-glutathionylated DsbM. The cysteinyl moiety of glutathione is covalently bound to the Cys14 residue and fits well to the $2F_o - F_c$ electron-density map (blue mesh). The interactions between glutathione and DsbM are represented by black dashes. Phe177 and Trp16 line the pocket containing the bound glutathione. (*c*) The reduced conformation of the C*XX*C motif. Cys14, which is located at the end of a long α-helix (α1), makes extensive interactions with the adjacent atoms, including bound water molecules (w1, w2 and w3). (*d*) The oxidized conformation of the C*XX*C motif. The distances between Cys14 and the amide groups of α1 are increased compared with the reduced conformation of the motif (*c*).

binding site holds a longer peptide with a cysteine residue. As mentioned above, the S-glutathionylated DsbM protein was created by incubation of reduced DsbM and oxidized glutathione with a disulfide bond between two glutathione molecules. Taken together, the glutathione-binding site of DsbM may also be involved in recognition of the oxidized peptide substrates.

3.6. Selective reduction of the disulfide bond of OxyR by DsbM

Although DsbM has been implicated in the reduction of oxidized OxyR in *P. aeruginosa* (Li *et al.*, 2014; Wang *et al.*, 2012), its role remains ambiguous. We found that the fluorescence from the tryptophan residue was highly quenched when the DsbM protein was oxidized, presumably because the disulfide bond in the C*XX*C motif quenched the fluorescence from Trp16 in the C*XX*C motif. Using the difference in the redox-dependent intensity of the fluorescence from tryptophan residues of DsbM, we measured the midpoint redox-potential value (E_m) of DsbM to obtain the thermodynamic basis for the reduction of OxyR by DsbM. From an experiment using a varying ratio of [GSH]/[GSSG], a value of −213 mV was derived, indicating a highly reductive potential of the protein. Since the redox potential of DsbM is much lower than that of OxyR (−185 mV; Zheng *et al.*, 1998; Fig. 5*a*), DsbM is capable of reducing OxyR thermodynamically.

To observe the direct interaction between DsbM and OxyR, we incubated the OxyR peptide containing a disulfide bond at Cys199 with the DsbM C17S mutant protein. The DsbM protein formed a disulfide intermediate with the OxyR peptide, as judged by the upshifted protein band on an SDS–polyacrylamide gel under nonreducing conditions (Fig. 5*b*). The DsbM–peptide complex was also confirmed by the quenched fluorescence (Fig. 5*b*). To obtain the selectivity of DsbM and to examine which cysteine residue(s) of OxyR is targeted by DsbM, we generated three single-cysteine-containing OxyR proteins. These OxyR proteins were made with only one cysteine residue (Cys25, Cys199 or Cys208) by changing the remaining cysteine residues of OxyR to serines. It was established that Cys199 and Cys208 of OxyR form a disulfide bond in response to elevated cellular H_2O_2 levels, whereas Cys25 is in the DNA-binding domain and is not involved in peroxide sensing (Choi *et al.*, 2001). The mutant proteins were incubated with DTNB to label each cysteine residue, resulting in TNB-labelled OxyR protein. We analyzed the reduction rate of each cysteine residue with the same concentrations of reduced DsbM or reduced glutathione. The results indicate that both Cys199 and Cys208 of OxyR are the main targets of DsbM and that OxyR is reduced more efficiently and rapidly by DsbM than by glutathione. Indeed, DsbM reduced 75% of the TNB-labelled Cys199 within the first 3 s of the reaction (Fig. 5*c* and Supplementary Fig. S3). Taken together, our observations indicate that DsbM reduces the Cys199–Cys208 disulfide bond of OxyR in *P. aeruginosa* with high selectivity and further suggests that DsbM is important in the rapid turn-off of the transcriptional activity of OxyR when cellular H_2O_2 levels decrease.

3.7. Complementary surface electrostatic potential between DsbM and OxyR

Based on our idea that DsbM reduces the disulfide of Cys199 and Cys208 in OxyR with high selectivity, we attempted to determine the structural implications of the

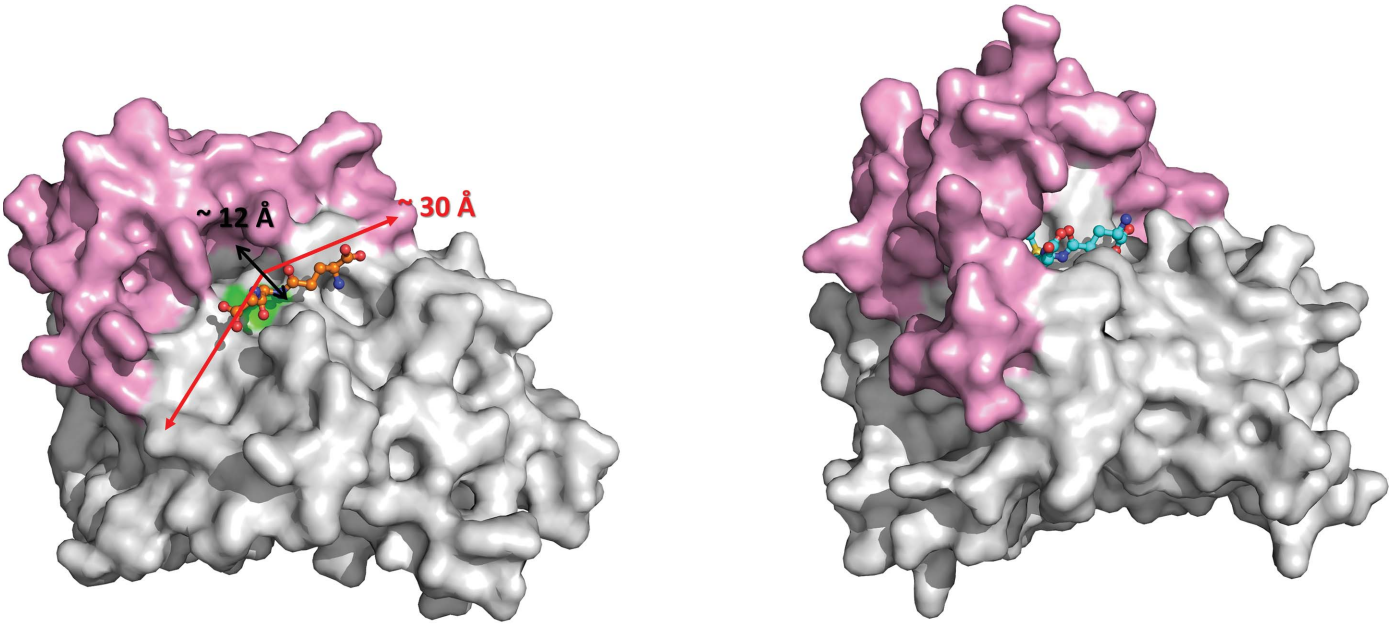

Figure 4
Structural comparison of the glutathione-binding sites of DsbM and hGST*κ*. The structures of S-glutathionyl DsbM (*a*) and glutathione-bound hGST*κ* (*b*) are displayed as surface representations (lid domain, pink; thioredoxin domain, grey; C*XX*C motif, green), whereas the glutathione molecules are shown as ball-and-stick representations. The dimensions of the shallow active site of DsbM are indicated.

preferential binding between DsbM and the inter-cysteine loop of OxyR (Cys199–Cys208). We analyzed the surface properties of the inter-cysteine loop region of oxidized OxyR (PDB entry 1i6a; Choi *et al.*, 2001). 20 positively charged amino acids were localized on one side of protein surface of DsbM (Fig. 6*a*). In contrast, a surface on the opposite side of DsbM was predominantly charged with electronegative potential (Supplementary Fig. S4*a*). In particular, electropositive patches of the α2–α3 helix (His57, His62, Arg65 and Arg84), Arg48 and the α7 helix (Arg159, Arg166, Arg167 and Arg171) surrounded the active site. Importantly, the electrostatic potential of the surface around the inter-cysteine loop of OxyR exhibited a strong negative charge, which was complemented by the positive electrostatic potential of the putative substrate-binding region of DsbM (Fig. 6*b* and Supplementary Fig. S4*b*). These findings can partly explain the preferential binding of OxyR by DsbM.

4. Discussion

In this study, we present crystal structures of DsbM, which acts in the bacterial cytoplasm. The S-glutathionylated DsbM structure revealed an extended glutathione-binding region which is structurally homologous to the glutathione-binding site of human GSTκ. The glutathione-binding region of DsbM can also hold a longer substrate peptide, such as the OxyR loop, which contains two conserved cysteine residues. Subsequent biochemical studies and structural analysis further support the ability of DsbM to reduce the disulfide of OxyR that is formed by H_2O_2.

Given the cellular location of DsbM, DsbM should acquire its reducing power from the cytosolic glutathione pool. Considering both the results in this paper and previously reported data on the reduction of DsbM by OxyR (Li *et al.*, 2014), we propose an mechanism of action for DsbM in which the oxidized OxyR and the reduced glutathione are shuttled on the glutathione-binding site (or putative substrate-binding region) of DsbM (Fig. 7). The reduced form of DsbM recognizes the oxidized inter-cysteine loop using the glutathione-binding region, forming an intermolecular disulfide bond between Cys14 of DsbM and Cys199 (or Cys208) of OxyR. Cys17 of DsbM resolves the intermolecular disulfide bond, forming a disulfide bond with Cys14 of DsbM and releasing the reduced form of OxyR. The first glutathione molecule reduces the disulfide bond of DsbM, resulting in a DsbM–glutathione covalent intermediate that is visualized in the S-glutathionylated DsbM structure. This intermediate structure is broken by another molecule of reduced glutathione,

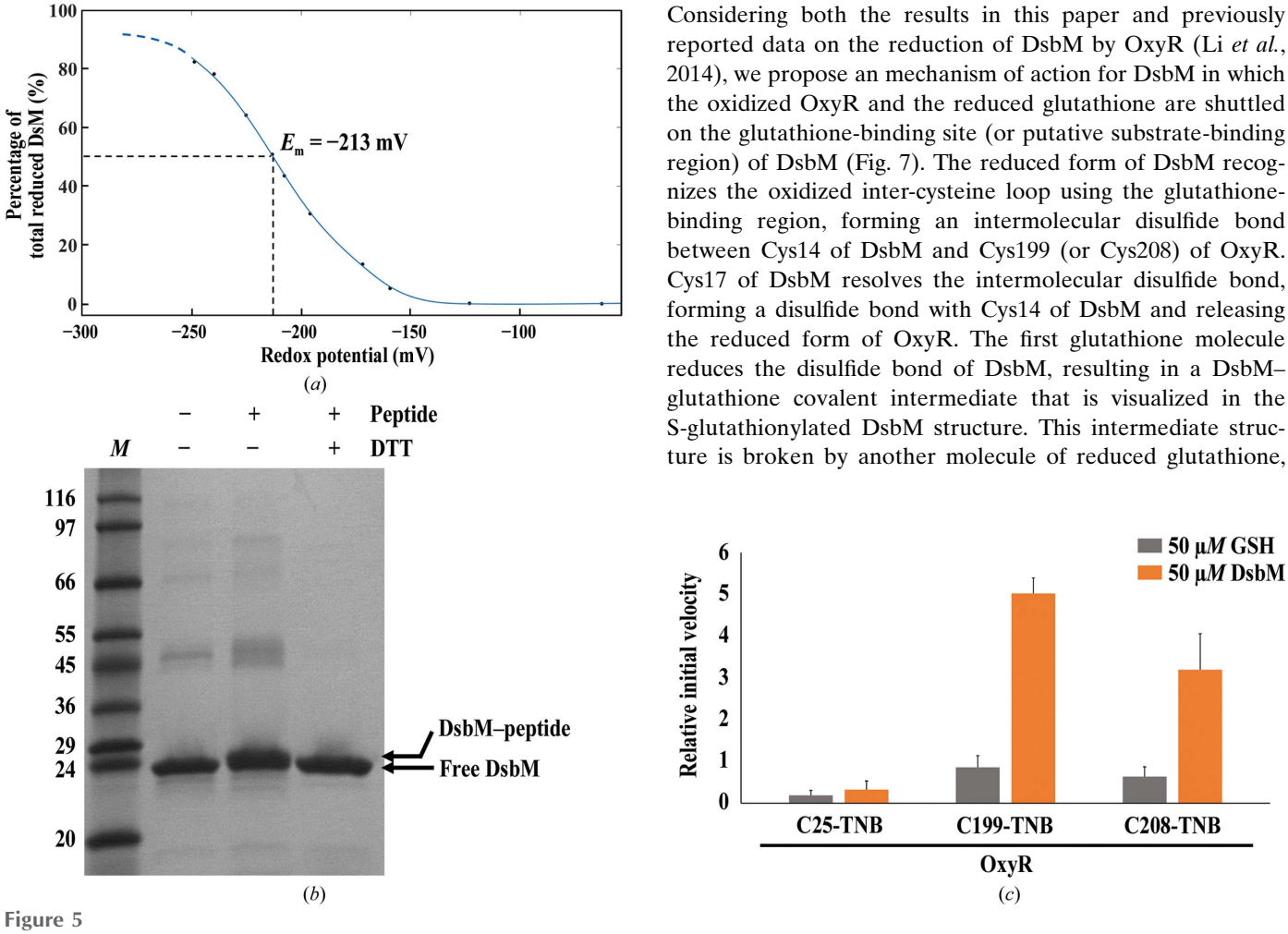

Figure 5
The reduction of OxyR by DsbM. (*a*) Midpoint redox-potential determination of DsbM. The titration was performed using various ratios of GSH/GSSG at 298 K in degassed buffer containing 50 m*M* Tris–HCl pH 7.0. The percentage of reduced DsbM was calculated from the tryptophan fluorescence. The midpoint redox potential of −213 mV is derived from three independent experiments (n = 3). (*b*) The DsbM C17S variant protein was incubated with a disulfidized OxyR peptide. The disulfidized peptide was prepared by linking two peptides (GHC^{199}FRDQVL) through an intermolecular disulfide bond at Cys199. A slight upshift of the DsbM band by the peptide is observed, indicating a covalent OxyR–DsbM intermediate. Lane *M* contains size markers (labelled in kDa). (*c*) Kinetic measurements of the thiol-reduction activity of DsbM C17S (orange bars) and the reduced glutathione (grey bars) with TNB-labelled OxyR variants (C25-TNB, C199-TNB and C208-TNB). Both DsbM C17S and GSH were at 50 μ*M* in 50 m*M* Tris–HCl pH 7.5 buffer containing 10 μ*M* TNB-labelled OxyR variant. The absorbance of the liberated TNB^{2-} was measured at 412 n*M*. The relative initial velocities were calculated from the slopes between 0 and 3 s. The initial value of reaction between 10 μ*M* OxyR (C199-TNB) and 50 μ*M* GSH is set as 1. The error bars indicate standard errors (n = 5).

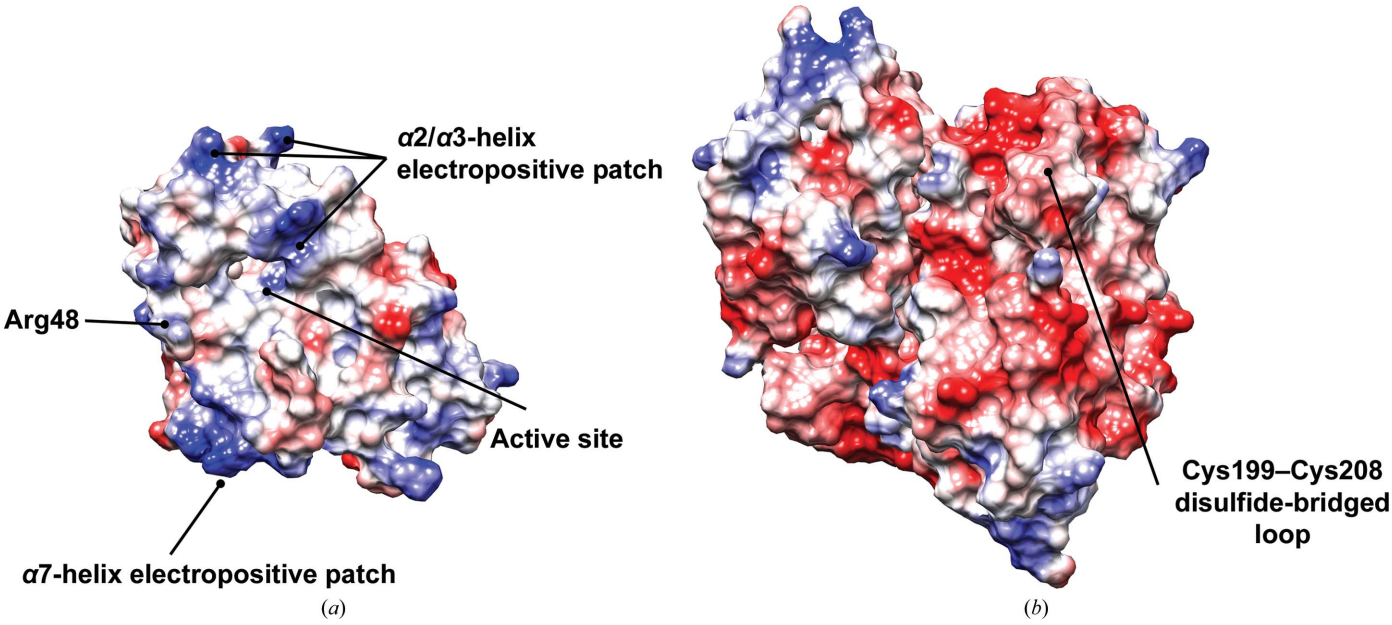

Figure 6
Comparison of the surface electrostatic potential of DsbM and OxyR. The solvent-accessible surface view of DsbM (*a*) and *E. coli*-oxidized OxyR (*b*) coloured by electrostatic potential as calculated with coulombic surface colouring in *Chimera* (Pettersen *et al.*, 2004). The potential contours are shown on a scale from −10.0 k_BT (red) to +10.0 k_BT (blue).

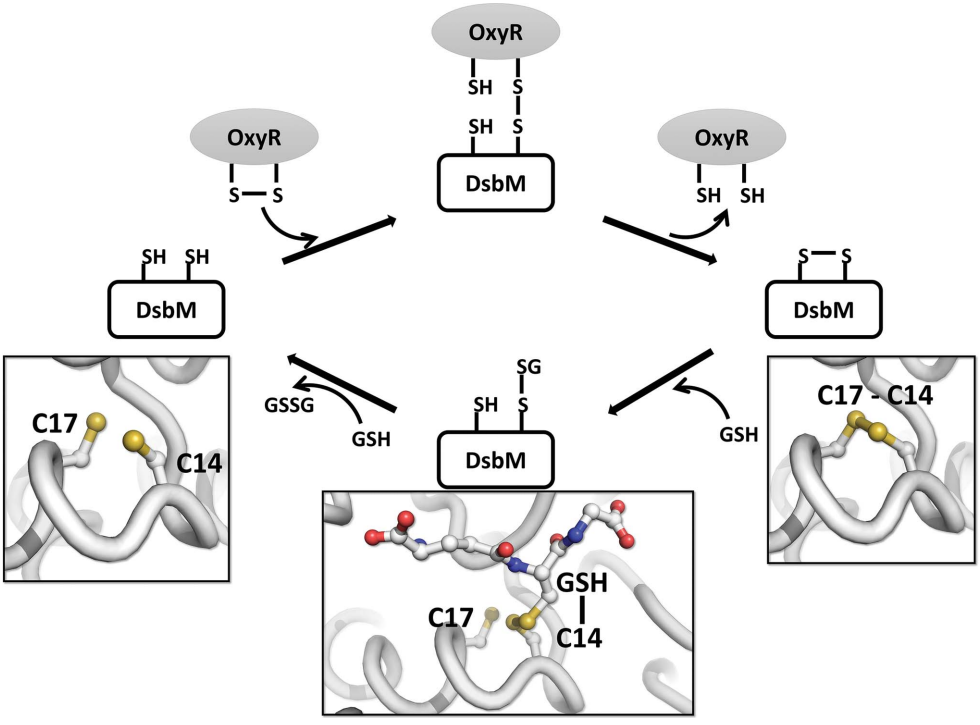

Figure 7
A proposed mechanism of action of DsbM. In the presence of oxidized OxyR, the Cys14 residue of the reduced DsbM attacks the disulfide bond of OxyR. The mixed-disulfide intermediate then reacts with the Cys17 residue of DsbM to form oxidized DsbM and reduced OxyR. The oxidized DsbM is glutathionylated by one GSH molecule. Another GSH molecule then reduces the S-glutathionylated DsbM.

producing a reduced form of DsbM and oxidized glutathione. DsbM is found in only a small portion of the bacteria that employ OxyR as a master H_2O_2-scavenging regulator (Li *et al.*, 2014; Wang *et al.*, 2012). It is known that oxidized OxyR is reduced by cellular glutathione in *E. coli*, which does not have *dsbM*, when reactive oxygen species stress is cleared (Zheng *et al.*, 1998). However, DsbM in *P. aeruginosa* appears to accelerate this reduction process, which is potentially related to rapid adaptation to changes in environmental stress.

The action of DsbC in the bacterial periplasm shows that the disulfide-bond reductase and isomerase helps in the correct folding of several proteins (Yeh *et al.*, 2007). DsbM has also been proposed to rearrange or isomerize the incorrect disulfide bond of a subset of proteins (Wang *et al.*, 2012). Given the highly reductive properties of DsbM, this disulfide-bond isomerase activity of DsbM is highly acceptable. However, further studies are required to clarify the role of DsbM in certain bacteria. In conclusion, we have studied the structural and biochemical aspects of the DsbM protein, and our findings have expanded understanding of the roles of redox-related proteins with a common C*XX*C motif in the cytosolic region of bacteria.

Acknowledgements

This research was supported by the R&D Convergence Center Support Program funded by the Ministry for Food, Agriculture, Forestry and Fisheries, Republic of Korea. We made use of beamline 5C at Pohang Accelerator Laboratory.

References

Afonine, P. V., Grosse-Kunstleve, R. W., Echols, N., Headd, J. J., Moriarty, N. W., Mustyakimov, M., Terwilliger, T. C., Urzhumtsev, A., Zwart, P. H. & Adams, P. D. (2012). *Acta Cryst.* D**68**, 352–367.
Charbonnier, J.-B., Belin, P., Moutiez, M., Stura, E. A. & Quéméneur, E. (1999). *Protein Sci.* **8**, 96–105.
Chim, N., Riley, R., The, J., Im, S., Segelke, B., Lekin, T., Yu, M., Hung, L. W., Terwilliger, T., Whitelegge, J. P. & Goulding, C. W. (2010). *J. Mol. Biol.* **396**, 1211–1226.
Choi, H.-J., Kim, S.-J., Mukhopadhyay, P., Cho, S., Woo, J.-R., Storz, G. & Ryu, S.-E. (2001). *Cell*, **105**, 103–113.
Ellgaard, L. & Ruddock, L. W. (2005). *EMBO Rep.* **6**, 28–32.
Ellman, G. L., Courtney, K. D., Andres, V. Jr & Featherstone, R. M. (1961). *Biochem. Pharmacol.* **7**, 88–95.
Grimshaw, J. P., Stirnimann, C. U., Brozzo, M. S., Malojcic, G., Grütter, M. G., Capitani, G. & Glockshuber, R. (2008). *J. Mol. Biol.* **380**, 667–680.
Heo, Y.-J., Chung, I.-Y., Cho, W.-J., Lee, B.-Y., Kim, J.-H., Choi, K.-H., Lee, J.-W., Hassett, D. J. & Cho, Y.-H. (2010). *J. Bacteriol.* **192**, 381–390.
Heras, B., Edeling, M. A., Schirra, H. J., Raina, S. & Martin, J. L. (2004). *Proc. Natl Acad. Sci. USA*, **101**, 8876–8881.
Heras, B., Shouldice, S. R., Totsika, M., Scanlon, M. J., Schembri, M. A. & Martin, J. L. (2009). *Nature Rev. Microbiol.* **7**, 215–225.
Holm, L. & Rosenström, P. (2010). *Nucleic Acids Res.* **38**, W545–W549.
Inaba, K. & Ito, K. (2008). *Biochim. Biophys. Acta*, **1783**, 520–529.
Ito, K. & Inaba, K. (2008). *Curr. Opin. Struct. Biol.* **18**, 450–458.
Jiao, L., Kim, J.-S., Song, W.-S., Yoon, B.-Y., Lee, K. & Ha, N.-C. (2013). *J. Struct. Biol.* **183**, 1–10.
Jo, I., Chung, I.-Y., Bae, H.-W., Kim, J.-S., Song, S., Cho, Y.-H. & Ha, N.-C. (2015). *Proc. Natl Acad. Sci. USA*, **112**, 6443–6448.
Jones, D. P. (2002). *Methods Enzymol.* **348**, 93–112.
Kortemme, T. & Creighton, T. E. (1995). *J. Mol. Biol.* **253**, 799–812.
Kurth, F., Duprez, W., Premkumar, L., Schembri, M. A., Fairlie, D. P. & Martin, J. L. (2014). *J. Biol. Chem.* **289**, 19810–19822.
Landt, O., Grunert, H. P. & Hahn, U. (1990). *Gene*, **96**, 125–128.
Lester, J., Kichler, S., Oickle, B., Fairweather, S., Oberc, A., Chahal, J., Ratnayake, D. & Creuzenet, C. (2015). *Mol. Microbiol.* **96**, 110–133.
Li, M., Guan, X., Wang, X., Xu, H., Bai, Y., Zhang, X. & Qiao, M. (2014). *FEMS Microbiol. Lett.* **352**, 184–189.
Martin, J. L. (1995). *Structure*, **3**, 245–250.
Otwinowski, Z. & Minor, W. (1997). *Method Enzymol.* **276**, 307–326.
Pettersen, E. F., Goddard, T. D., Huang, C. C., Couch, G. S., Greenblatt, D. M., Meng, E. C. & Ferrin, T. E. (2004). *J. Comput. Chem.* **25**, 1605–1612.
Qi, Y. & Grishin, N. V. (2005). *Proteins*, **58**, 376–388.
Schafer, F. Q. & Buettner, G. R. (2001). *Free Radic. Biol. Med.* **30**, 1191–1212.
Shouldice, S. R., Heras, B., Walden, P. M., Totsika, M., Schembri, M. A. & Martin, J. L. (2011). *Antioxid. Redox Signal.* **14**, 1729–1760.
Shukla, J., Gupta, R., Thakur, K. G., Gokhale, R. & Gopal, B. (2014). *Acta Cryst.* D**70**, 1026–1036.
Storz, G. & Tartaglia, L. A. (1992). *J. Nutr.* **122**, 627–630.
Toledano, M. B., Kullik, I., Trinh, F., Baird, P. T., Schneider, T. D. & Storz, G. (1994). *Cell*, **78**, 897–909.
Tu, B. P. & Weissman, J. S. (2004). *J. Cell Biol.* **164**, 341–346.
Um, S.-H., Kim, J.-S., Lee, K. & Ha, N.-C. (2014). *Acta Cryst.* F**70**, 1167–1172.
Um, S.-H., Kim, J.-S., Song, S., Kim, N. A., Jeong, S. H. & Ha, N.-C. (2015). *Mol. Cells*, **38**, 715–722.
Wang, X., Li, M., Liu, L., Mou, R., Zhang, X., Bai, Y., Xu, H. & Qiao, M. (2012). *J. Microbiol.* **50**, 932–938.
Wang, B., Peng, Y., Zhang, T. & Ding, J. (2011). *Biochem. J.* **439**, 215–225.
Winn, M. D. *et al.* (2011). *Acta Cryst.* D**67**, 235–242.
Yeh, S.-M., Koon, N., Squire, C. & Metcalf, P. (2007). *Acta Cryst.* D**63**, 465–471.
Yoon, B.-Y., Kim, J.-S., Um, S.-H., Jo, I., Yoo, J.-W., Lee, K., Kim, Y.-H. & Ha, N.-C. (2014). *Biochem. Biophys. Res. Commun.* **446**, 971–976.
Yoon, J. Y., Kim, J., Lee, S. J., Kim, H. S., Im, H. N., Yoon, H.-J., Kim, K. H., Kim, S.-J., Han, B. W. & Suh, S. W. (2011). *FEBS Lett.* **585**, 3862–3867.
Zheng, M., Aslund, F. & Storz, G. (1998). *Science*, **279**, 1718–1721.